ELSEVIER

Ceramics International 29 (2003) 841–846

CERAMICS INTERNATIONAL

www.elsevier.com/locate/ceramint

# Microstructural characterization of gas-pressure-sintered α-silicon nitride containing β-phase seeds

Chien-Cheng Liu*

*Department of Mechanical Engineering, Kun Shan University of Technology, No.949, Da Wan Rd., Yung-Kang City, Tainan Hsien 710, Taiwan, ROC*

Received 29 November 2002; received in revised form 12 December 2002; accepted 5 January 2003

**Abstract**

The starting α-$Si_3N_4$ powders with or without the addition of β-phase seeds using $Y_2O_3$ and $Al_2O_3$ as sintering aids were gas-pressure-sintered with the conditions, 0.9 MPa nitrogen gas at 1850 °C for 1 h. The microscopic evidence indicates that β-$Si_3N_4$ seeds incorporated in the starting α-$Si_3N_4$ powders play an important role in microstructural development and mechanical properties for silicon nitride. The growth of β-$Si_3N_4$ grains is initiated from the seeds, resulting in a core/shell microstructure was observed in the abnormal grain growth. As a result, the fracture toughness of silicon nitride was improved from 5.5 to 7.6 MPa $m^{1/2}$ by adding β-phase seeds.


*Keywords:* B. Microstructure; D. Silicon nitride; Seeds

## 1. Introduction

Silicon nitride is an attractive ceramic material because of its excellent mechanical properties at both ambient and elevated temperatures. Therefore, it has been widely used for structural applications, such as cutting tools, mechanical sealing, bearings, heat exchangers, components for heat engines and in chemically corrosive environments [1,2]. The high fracture toughness that is observed in silicon nitride ceramics is attributed to the needlelike grain morphologies that are evidenced in the microstructure. Tailoring of the $Si_3N_4$ microstructure is possible via the inclusion of β- $Si_3N_4$ seeds in the initial sintering composition [3]. The β- $Si_3N_4$ powder was gas-pressure sintered at 2000 °C for 2–8h in 30 MPa nitrogen gas. These materials had a microstructure of "in-situ composites" as a result of exaggerated grain growth of some β- $Si_3N_4$ grains during firing [4]. Typical fracture toughness values of silicon nitrides obtained by pressureless sintering are in the range of 4–6 MPa $m^{1/2}$. By seeding morphological regulated particles, fracture toughness of silicon nitride was improved from 6.3 to 8.4–8.7 MPa $m^{1/2}$, retaining high strength levels of about 1 GPa [5]. Kleebe et al., reported on the effect of grain boundary phase. The grain-boundary microstructure and interface chemistry of $Yb_2O_3/Al_2O_3$ fluxed sintered $Si_3N_4$ materials with and without the addition of CaO has effected the grain boundary width [6]. The amorphous phase of grain boundary still limited material properties such as mechanical strength, creep resistance, thermal conductivity and high temperature properties. The α-β transformation of silicon nitride has occurred in presence of a liquid phase and the solution-precipitation mechanism dominant [7]. The incorporated β-$Si_3N_4$ seeds played an essential role in the heterogeneous grain growth of β- $Si_3N_4$ grains and clearly observed the core/shell structure [8].

In this study, we investigated the effect of addition β-$Si_3N_4$ seeds. Image analysis, transmission electron microscopy (TEM) and scanning electron microscopy (SEM) were using for analyzing the effect of β-$Si_3N_4$ seeds on the microstructure. The flexural strength and fracture toughness were also investigated.

## 2. Experimental procedure

### 2.1. Materials fabrication

The $Si_3N_4$ (UBE SN-E10) powder was mixed with 2 wt.%$Al_2O_3$ (16SG,Alcoa, USA, 0.5 μm ), 6 wt.%$Y_2O_3$

* Tel.: +886-6-2050783.
*E-mail address:* liu@mail.ksut.edu.tw (C.-C. Liu).

0272-8842/03/$30.00 
doi:10.1016/S0272-8842(03)00027-0

(5603, Molycorp, USA, 1.8 μm ) and the β-$Si_3N_4$ (Cerac; S-1177, 0.74 μm ) in a polyurethane bottle with high-purity silicon nitride balls and ethanol for 24 h. The ratio of ball, charge and vehicle was 6:1:5 in weight. It was dried in a rotary evaporator. Dried agglomerates were ground with a mortar and pestle, and passed through a 200 meshes sieve to pulverize aggregates. Samples were gas-pressure sintered with the conditions, 0.9 MPa nitrogen gas at 1850 °C for 1 h in a graphite furnace (Fuji Dempa High Multi 5000).

### 2.2. Microstructural analysis

Flexural strength was measured by a four-point bending test on a universal testing machine (Instron 8511) at a loading rate of 0.5 mm/min. Testing samples were machined into bars with dimensions of 3.5×4.5×45 mm and polished to 15 μm. The inner and outer spans used were 20 and 40 mm, respectively. Fracture toughness was measured following the derivation of Evans and Charles [9] by the indentation technique.

TEM foil preparation was performed by standard techniques which include diamond cutting, ultra-sound drilling, mechanical grinding, dimpling, ion thinning to perforation, and a light carbon coating. An energy dispersive spectrometer (EDS) associated with TEM was employed for elemental analysis, and high resolution electron microscopy (HREM) images were taken (Model: Jeol-3010) operating at 300 kv. A scanning electron microscope (Hitachi S-4100) was employed to examine the microstructure. Some samples were plasma etched (Plasma-Them Inc., Series 70) in gas mixtures of $CF_4$ and $O_2$ with a flow ratio of 93:7 in RF sputtering system for 2 min and then ultrasonically cleaned prior to examination by SEM. The size distribution of grains was measured by an image analyzer associated with OPTIMAS (Bioscan Inc., Edmons, Washington USA) and was calculated following the statistical derivation by Woetting et al. [10].

## 3. Results and discussion

Typical SEM micrographs of $Si_3N_4$ containing different amount of β-$Si_3N_4$ seeds are shown in Fig. 1. Samples had a compound microstructure composed of small matrix grains and large elongated grains. As revealed by Fig. 1(b–d), the number of large grains increases con-

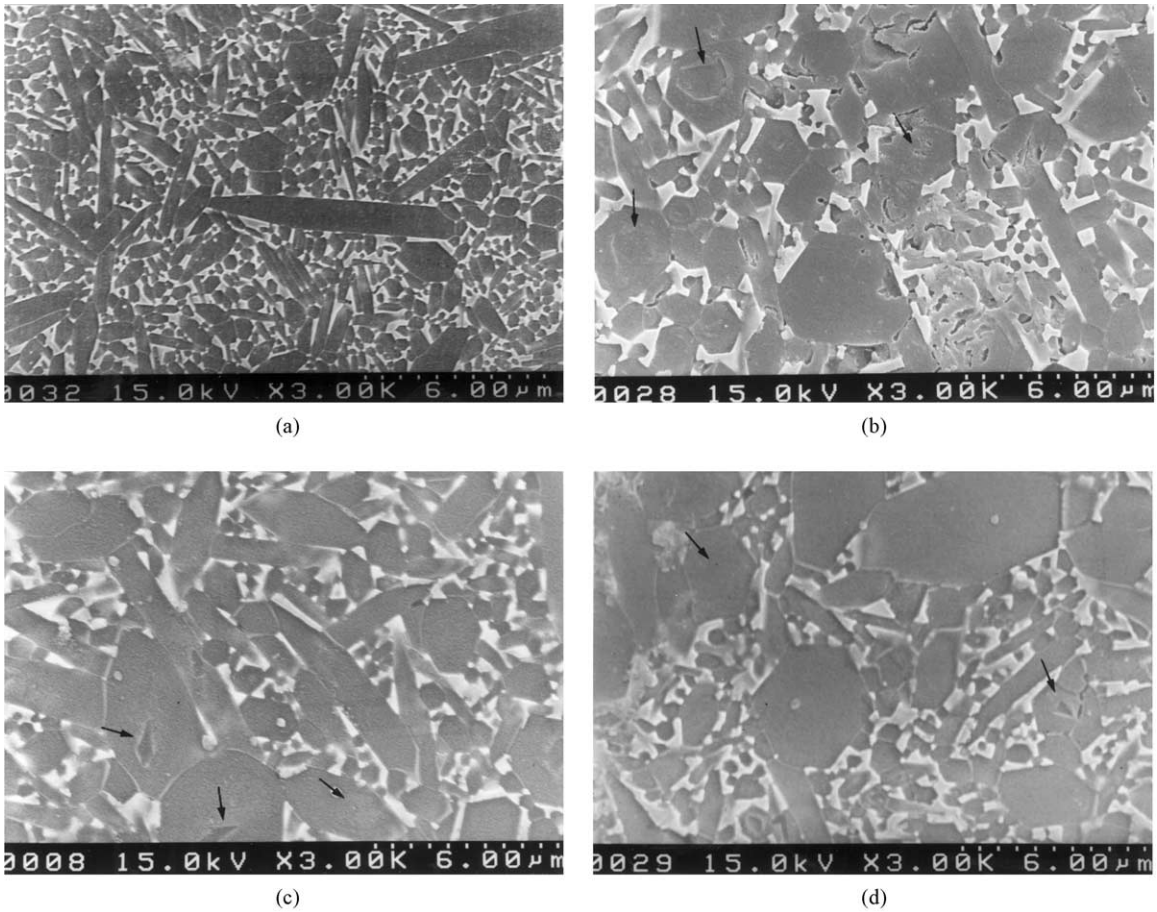


Fig. 1. Microstructure of $Si_3N_4$ ceramics with (a) 0 wt.%β-$Si_3N_4$, (b) 2 wt.%β-$Si_3N_4$, (c) 5 wt.%β-$Si_3N_4$, and (d) 7 wt.%β-$Si_3N_4$. Samples were sintered at 0.9 MPa nitrogen gas at 1850 °C for 1 h.

sistently with a small amount of seeds. These sintered samples also showed biomodal microstructure with large grains in the fine matrix grains. The average grain diameters of β-$Si_3N_4$ indicate a trend of increase in grain size with the amount of seeds. These results are shown in Fig. 2. With seed grain size distribution patterns were complex which compared without seed of the sintered samples. Emoto et al. [11] reported, the grain growth of α- $Si_3N_4$ is through the solution process of liquid phase sintering and subsequent precipitation of β-phase in additive β-$Si_3N_4$ seeds. These seeds should act as nuclei for grain growth. It was formerly discussed that a large diameter and elongated grains exhibit a core/rim structure, in which the growth of β-grains is initiated from the β-seeds [8]. Hirosaki et al. [12] have proposed that the elongated grains in the materials with seeds had a larger diameter and a smaller aspect ratio than without seeds. A core/rim structure was observed in the elongated grains.

The flexural strength slightly decreased with addition β-phase seeds, because of the large elongated grains in the matrix possibly being effected. Fracture toughness progressively increases with the addition of β-$Si_3N_4$ seeds, as shown in Fig. 3, from 5.5 $MPa^{1/2}$ for without seeds $Si_3N_4$, to between 6.5 and 7.5 $MPa^{1/2}$ for 7 wt.% β-$Si_3N_4$ seeds. The elongated grains of β-$Si_3N_4$ can be formed in situ reinforced monolithic silicon nitride. Becher et al. [13] have proposed that with the addition of 2% rodlike seeds, the fracture resistance can be increased due to bimodal grain diameter distribution. However, a larger amount seeds gave improvement in fracture toughness. The increased fracture toughness may be related to the bimodal microstructure, which is ascribed to grain bridging and crack deflection. Faber et

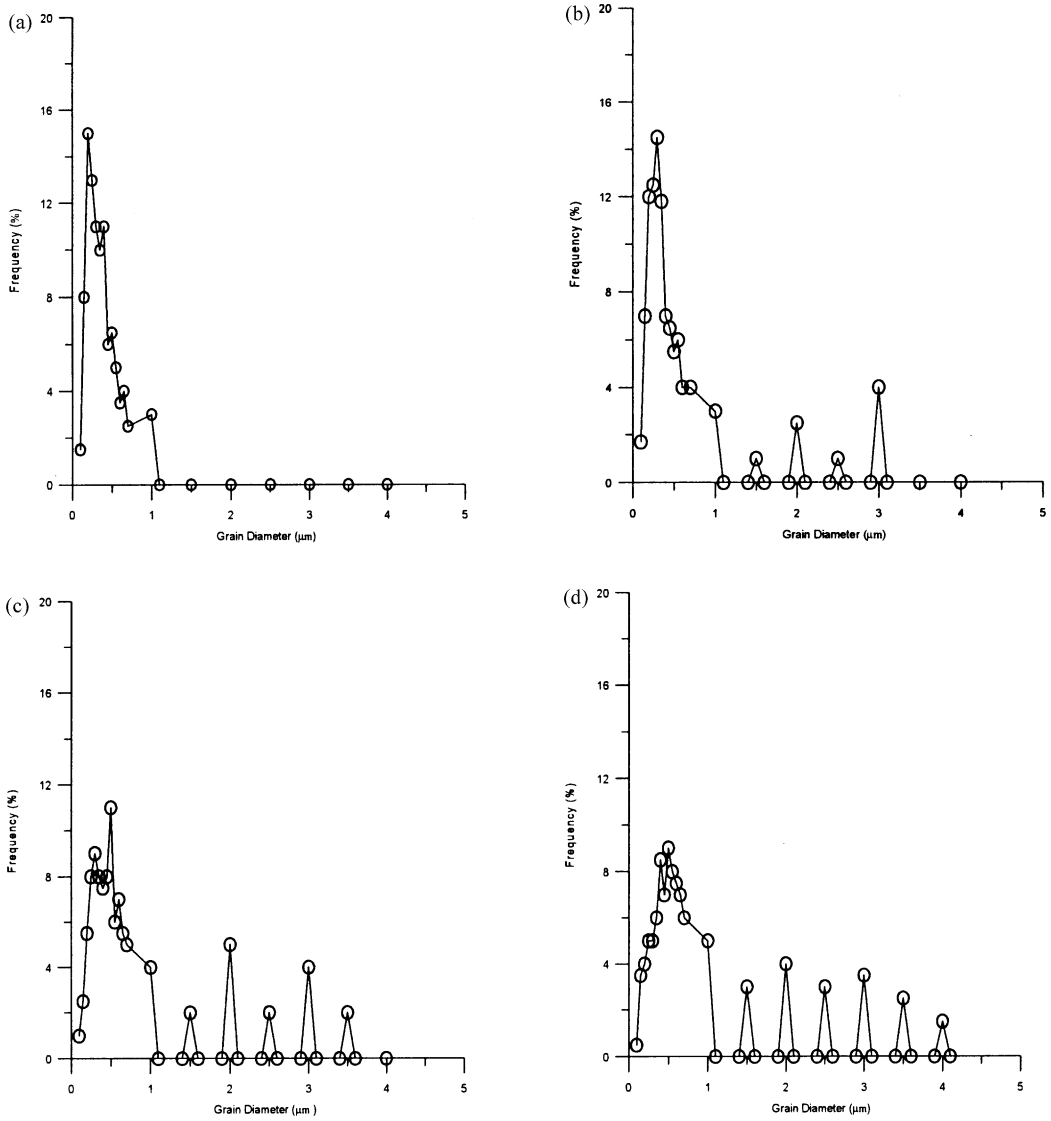


Fig. 2. Grain diameter distribution of $Si_3N_4$ containing different amount of β-$Si_3N_4$: (a) 0 wt.% seed, (b) 2 wt.% seed, (c) 5 wt.% seed, (d) 7 wt.% seed. Samples were sintered at 0.9 MPa nitrogen gas at 1850 °C for 1 h.

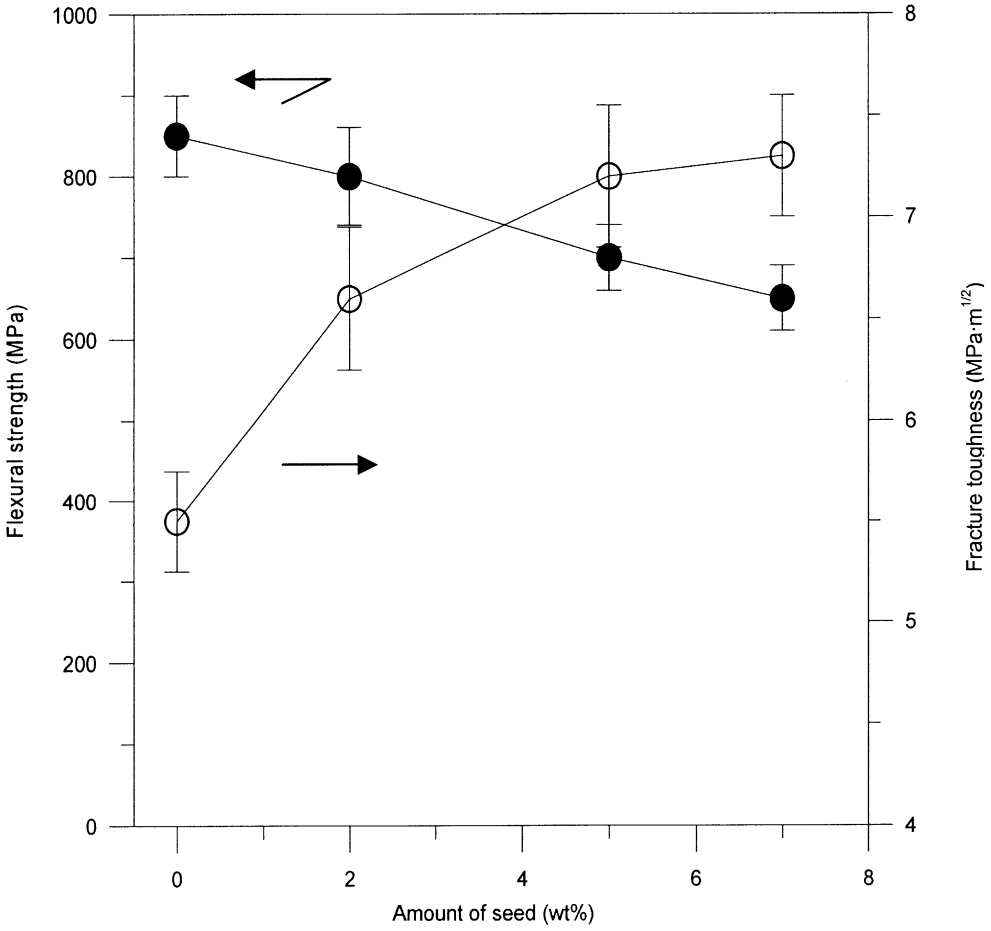


Fig. 3. Mechanical properties of silicon nitride sintered at 1850 °C for 1 h as a function of amounts of β-seed.

al. [14] have reported that the fracture toughness increased due to crack deflection around second phase particles. The most effective morphology for deflecting propagating cracks in the rod of high ratio. Ohashi et al. [15] Pointed out that the intergranular fracture of liquid phase sintered ceramics is dependent on the thermal residual stress in the vicinity of the intergranular phase.

SEM analysis showed that those with seeds have a bimodal microstructure and large columnar grains, i.e., coarse elongated grains within a fine grain matrix. Observation of the Vickers indentation crack introduced on a polished surface revealed that the crack was deflected by β-$Si_3N_4$ columnar particles. Fig. 4 shows the travel of a Vickers indentation crack. It is clear that the crack traveled around the β-$Si_3N_4$ grains, which the crack deflected and branched at points "B" and "C". However, this is clear evidence of crack deflection so that more energy is absorbed during fracture of the β-$Si_3N_4$ columnar grains. It was suggested that the crack propagation resistance is increased by both the crack deflection and bridging dominant. This finding is consistent with results reported by Kleebe et al., who indicate that the toughening contribution from crack bridging strongly increases with an increase in larger elongated β-$Si_3N_4$ grains [16].

Fig. 5(a) shows the sintered sample, the amorphous film had a constant thickness along the entire grain boundary and in triple-grain junctions. For structural analysis of the amorphous, it has been reported that the average film thickness was 0.99 nm with a standard deviation of ±0.1 nm [17]. The reduction in strength is due to softening at elevated temperature. On the other hand, the high resolution TEM image of the core/shell interface is shown in Fig. 5(b). The lattice image indicates that the core and shell do not have an amorphous phase in the interface. The lattice planes suggested a coherence between the core and the shell, which showed the same orientation and degree. The separation of the lattice planes was 0.659 nm, corresponding to a (100) plane of β-$Si_3N_4$. The core is a β-$Si_3N_4$ seed, which acts as a nucleus during liquid phase sintering. The aluminum concentration in the core was apparently much greater than that in the shell [18]. The dark contrast and lattice fringe shift at the core/rim boundary were attributed to an elastic strain caused by a mismatch of the lattice spacing [13].

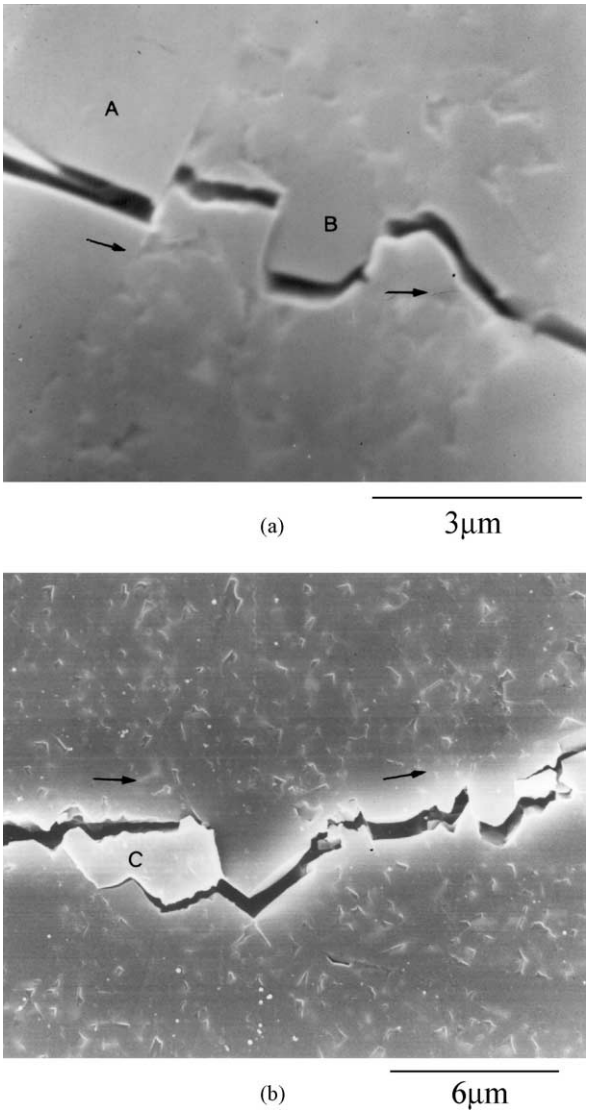


Fig. 4. SEM micrographs of Vickers indentation crack propagation paths with 2 wt.% seeds: (a) cracking bridging and (b) crack branching.

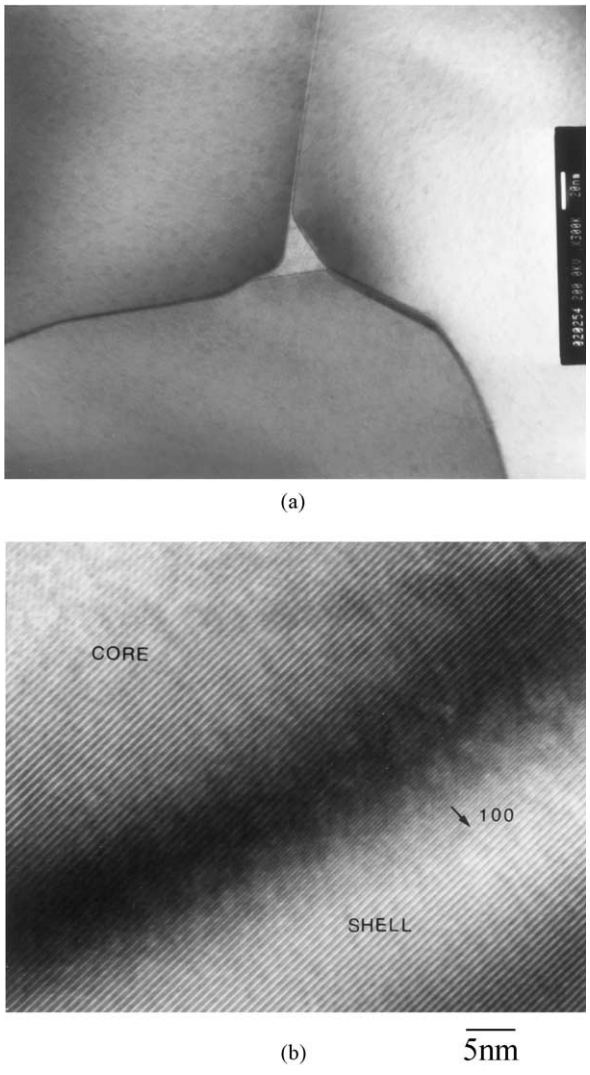


Fig. 5. TEM lattice image of silicon nitride showing (a) grain-boundary amorphous phase, and (b) lattice image of the core and shell structure.

## 4. Conclusion

1. The SEM micrograph shows that improvement of fracture toughness was directly related to the biomodal microstructure with large grains in the fine matrix grains, which arose from crack bridging and deflection interaction. This crack deflection mechanism played an important role in the toughening effects.
2. The average grain diameters of β-$Si_3N_4$ indicate a trend of increase in grain size with the amount of seeds.
3. The grain-boundary amorphous film was shown along the entire grain boundary and in triple-grain junctions.
4. The lattice image shows a coherence match between the core and the shell boundary.

## Acknowledgements

The authors would like to thank the National Science Council of the R.O.C. for its financial support under the contract No. NSC89-2216-E-168-001.

## References

[1] J.L. Huang, S.Y. Chen, M.T. Lee, Microstructure, chemical aspects, and mechanical properties of $TB_2/Si_3N_4$ and TiN/ $Si_3N_4$ composites, J. Mater. Res. 9 (9) (1994) 2349–2354.
[2] D.F. Lii, J.L. Huang, C.H. Lin, H.H. Lu, The effect of atmosphere on the thermal debinding of injection moulded $Si_3N_4$ components, Ceram. Int. 24 (1998) 99–104.
[3] P.D. Ramesh, R. Oberacker, M.J. Hoffmann, Preparation of β-silicon nitride seeds for self-reinforced silicon nitride ceramics, J. Am. Ceram. Soc. 82 (6) (1999) 1608–1610.

[4] N. Hirosaki, Y. Akimune, Effect of grain growth of β-silicon nitride on strength, Weibull modulus, and fracture toughness, J. Am. Ceram. Soc. 76 (7) (1993) 1892–1894.
[5] K. Hirao, T.N. Agaoka, M.E. Brito, S. Kanzaki, Microstructure control of silicon nitride by seeding with rodlike β-silicon nitride particles, J. Am. Ceram. Soc. 77 (7) (1994) 1857–1862.
[6] H.J. Kleebe, J. Bruley, M. Ruhle, HREM and AEM studies of $Yb_2O_3$-fluxed silicon nitride ceramics with and without CaO addition, J. Eur. Ceram. Soc. 14 (1994) 1–11.
[7] T.E. Mitchell, J.J. Petrovic, The α–β transformation in silicon nitride single crystals, J. Am. Ceram. Soc. 88 (3) (1997) 615–620.
[8] H.H. Lu, J.L. Huang, Microstructure in silicon nitride containing β-phase seeding: III, grain growth and coalescence, J. Am. Ceram. Soc. 84 (8) (2001) 1891–1895.
[9] A.G. Evans, E.A. Charles, Fracture toughness determinations by indentation, J. Am. Ceram. Soc. 59 (7-8) (1976) 371–376.
[10] G. Woetting, B. Kanka, G. Ziegler, in: S. Hampshire (Ed.), Non-Oxide Technical and Engineering Ceramics, Elsevier Applied Science, London, York, 1986, pp. 83.
[11] H. Emoto, H. Hirotsuru, Microstructure control of silicon nitride ceramics fabricated from α-powder contqining fine β-nuclei, J. Ceram. Soc. Jpn. 161–163 (2) (1999) 469–474.
[12] N. Hirosaki, Y. Akimune, Microstructure characterization of gas-pressure sintered β-silicon nitride containing large β-silicon nitride seeds, J. Am. Ceram. Soc. 77 (4) (1994) 1093–1097.
[13] P.F. Becher, E.Y. Sun, K.P. Plucknett, K.B. Alexander, C.H. Hsueh, H.T. Lin, S.B. Waters, C.G. Westmoreland, Microstructure design of silicon nitride with improved fracture toughness: I, effects of grain shape and size, J, Am. Ceram. Soc. 81 (11) (1998) 2821, - 2830.
[14] K.T. Faber, A.G. Evans, Crack deflection processes—I. Theory, Acta. Metall. 31 (4) (1983) 565–576.
[15] M. Ohashi, K. Nakamura, K. Hirao, M. Toriyama, S. Kanzaki, Factors affecting mechanical properties of silicon oxynitride ceramics, Ceram. Int. 23 (1997) 27–37.
[16] H.J. Kleebe, G. Pezzotti, G. Ziegler, Microstructure and fracture toughness of $Si_3N_4$ ceramics: combined roles of grain morphology and secondary phase chemistry, J. Am. Ceram. Soc. 82 (7) (1999) 1857–1867.
[17] Q. Jin, D.S. Wilkinson, G.C. Weatherly, High-resolution electron microscopy investigation of viscous flow creep in a high-purity silicon nitride, J. Am. Ceram. Soc. 82 (6) (1999) 1492, -1496.
[18] H.H. Lu, J.L. Huang, Microstructure in silicon nitride containing β-phase seeding: part I, J. Mater. Res. 14 (7) (1999) 2966–2973.